

Article

Effects of Temperature and Solar Irradiation Variations on The Performances of Photovoltaic Pumping Systems

Moncef Jraidi and Adnen Cherif 

Laboratory of Electric and Energetic Systems, Science faculty of Tunis, University Tunis Manar, 2092 Tunis, Tunisia

* Correspondence: adnen2fr@yahoo.fr

Received: 28 March 2024; **Revised:** 7 May 2024; **Accepted:** 17 May 2024; **Published:** 14 June 2024

Abstract: Climate and solar radiation levels are two major environmental elements that affect the operation of photovoltaic (PV) pumping systems. Rising temperatures cause a decrease in PV modules' electrical efficiency because of the fall of fill factor and open-circuit voltage. They may also cause a decrease in motor efficiency because of the growing winding resistance losses. Besides, the increased photocurrent and power production of the PV array are caused by higher levels of solar irradiation, which makes the pump run at higher speeds or flow rates. To quantify these impacts and forecast system performance, precise modeling techniques and control laws are used such as MPPT, PWM and U/F in this paper. This paper presents solar performances and responses such as the flow of the pumped water, the PV power outputs, motor voltages, currents, speed and finally converter controls. However, although MPPT and PWM control laws improve the energy efficiency of the overall system, the simulation results show that the performance of the PV pumping system degrades when the temperature increases and the solar flux decreases, which will affect the autonomy of the PV system.

Keywords: standalone PV system; solar pumping; modeling and simulation of MPPT and PWM controls

1. Introduction

The first work on photovoltaic pumping systems can be traced back to the 1970s, when researchers were investigating these systems' feasibility and potential applications, particularly for water pumping in remote and off-grid areas [1,2]. Early studies focused on the basic characteristics and performance evaluation of photovoltaic pumping systems under various environmental conditions. The main problems and challenges discussed in these studies are the intermittence behavior and fluctuations of renewable energy sources.

Actually, the deployment of rural photovoltaic pumping systems faces other challenges in the initial cost and affordability, sizing and design, technical expertise and maintenance, energy storage, and system reliability. To analyze the hydraulic performance of pumps in photovoltaic pumping systems, researchers used affinity laws [3,4] and empirical pump curves [5,6] to correlate flow rate and power consumption. The effects of solar irradiation on the available electrical energy of the photovoltaic array were integrated to predict the operating point and performance of the pump. Then researchers focused on the development of integrated models combining models of photovoltaic generators, powerconverters, motors and pumps [7,8]. These models achieved system-level simulations and optimizations, considering factors such as size and control strategies. Numerous field experimental studies have been conducted under various environmental conditions to validate these mathematical models. These studies provided valuable data for model refinement and optimization [9].

In recent years, researchers have explored advanced techniques to improve the modeling and optimization of photovoltaic pumping systems. This includes the use of artificial intelligence and machine learning techniques, <https://doi.org/10.54963/nea.v3i1.244>

as well as the incorporation of advanced control strategies and energy storage systems to improve system performance and reliability [10]. In fact, the output power of the PV panels depends on several climatic factors such as solar irradiation, ambient temperature and condition of the solar panels (aging, cleanliness, etc.). These parameters have a significant impact on the performance and behavior of the solar plants. The realization of an autonomous pumping system, with high efficiency and reliability, is a practical and economical way to solve the water shortage problem in desert and rural areas.

This paper will present the responses and the parameters of a standalone PV pumping plant under several climatic conditions and disturbances. We will also develop the global model of the solar system with mechanical pumping [11] as well as the control laws of DC-DC and DC-AC converters. We will study closely the influence of temperature changes and solar irradiation on the output performance of the system and, especially on the pumping flow rate. Simulation results are also illustrated under different levels of solar irradiation and temperature. These two setting parameters will be considered disruptive to the overall system composed of a PV generator, a power adapter/converter, a voltage inverter and a submerged pump.

2. Modeling of the PV Pumping System

In Figure 1, the system consists of a PV generator, a power converter DC/DC which is controlled by MPPT (Maximum Power Point Tracking), an inverter DC/AC which is controlled by PWM and finally a submersed centrifugal pump composed of a three-phase asynchronous motor.

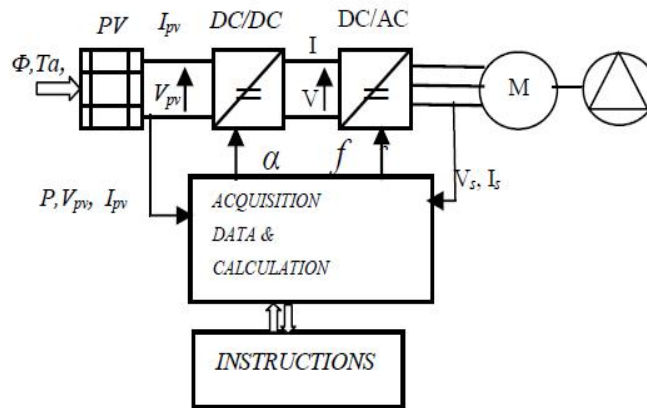


Figure 1. Overall Structure of PV pumping system.

2.1. The PV Generator

The model used for the simulation of the PV generator is a single-diode model [12], which is described by the relationship between the current I_{PV} and the voltage V_{PV} , as follows in Equation (1):

$$I_{PV} = I_{PH} - I_S \left[\exp^{\frac{q}{n k T} (V_{PV} + I_{PV} R_S)} - 1 \right] - (V_{PV} + I_{PV} R_S) \times \frac{1}{R_{Sh}} \quad (1)$$

The parameters of the model are determined through experiments for an AEG PV generator. For weather data (solar radiation, temperature, and wind speed) flows, this model is used to calculate the characteristic curve: PV current in the function of the PV: voltage $I_{PV} = f(V_P)$.

2.2. The Inverter

The photovoltaic pumping is monitored by an off-grid inverter as used in rural farms. From DC voltage, it provides a three-phase voltage system with variable amplitude and frequency, which may operate an induction motor at any speed within the range from 0.1 to 1 times the nominal frequency.

The model of the inverter with its control PWM, developed under MATLAB/SIMULINK, is presented by the system of equations in three output voltages as follows in Equation (2) [13]:

$$\begin{pmatrix} v_{as} \\ v_{bs} \\ v_{cs} \end{pmatrix} = \begin{pmatrix} 2 & -1 & -1 \\ -1 & 2 & -1 \\ -1 & -1 & 2 \end{pmatrix} \begin{pmatrix} c1 \\ c2 \\ c3 \end{pmatrix} \quad (2)$$

where $c_i = \{0 \text{ or } 1\}$; For $i = \{1,2,3\}$, represent control signals of the PWM inverter; 0: the low level control = 0 V; 1: the high level control = 5 V.

The PWM signal is generated at a frequency of 2000 Hz in order to eliminate the low harmonics 3, 5, 7 and 11. The high order harmonics are filtered by the inductance of the machine. The shape of the output voltage is sinusoidal with a low distortion rate (2%).

2.3. The Electric Motor

It is a three-phase asynchronous motor, which is the most appropriate type for pumping PV systems. The simulation model is chosen as the template phase [14]. It is defined by the voltage equations of the stator and rotor as follows in Equation (3):

$$\begin{aligned} v_{as} &= r_s i_{as} \left(\frac{d\phi_{as}}{dt} \right); v_{ar} = r_r i_{ar} + \left(\frac{d\phi_{ar}}{dt} \right) \\ v_{bs} &= r_s i_{bs} \left(\frac{d\phi_{bs}}{dt} \right); v_{br} = r_r i_{br} + \left(\frac{d\phi_{br}}{dt} \right) \\ v_{cs} &= r_s i_{cs} \left(\frac{d\phi_{cs}}{dt} \right); v_{cr} = r_r i_{cr} + \left(\frac{d\phi_{cr}}{dt} \right) \end{aligned} \quad (3)$$

According to reference [5], The electromagnetic couple is given by the following Equations (4) and (5):

$$C = \frac{1}{2} p M \left[i_{as} i_{br} \sin \left(\theta - \frac{2\pi}{3} \right) + i_{bs} i_{ar} \sin \left(\theta - \frac{4\pi}{3} \right) - (i_{as} i_{ar} + i_{bs} i_{br}) \sin (\theta) \right] \quad (4)$$

According to the fundamental relationship of the dynamic behavior, the motor's rotation speed N is given as follows:

$$C - Cr = J \frac{d\Omega}{dt} \quad (5)$$

The developed model of the pump allows for the calculation of the flow rate at each speed of the rotation provided by the machine based on the speed-height Equation (6):

$$H_n = a_0 W^2 + a_1 W Q + a_1 Q^2 \quad (6)$$

Or the speed of the motor can be expressed by the Equation (7):

$$w = (1 - w_r/w_s) w_s \quad (7)$$

The overall efficiency of the pump is expressed as a function of the height of the manometric level H_n , the flow rate Q , the speed N and the torque Cr as follows [14] in Equations (8)–(11):

$$\eta = \frac{wQH_n}{2\pi NCr} \quad (8)$$

$$Cr = \frac{w}{2\pi g} Q(\eta_0 N - \lambda_1 Q) \quad (9)$$

$$\lambda_1 = \frac{\lambda_0}{\tan(\beta/2)} \quad (10)$$

$$H_n = \eta N^2 + NQ + KQ^2 \quad (11)$$

where, λ_1 and K are coefficients, which depend on the geometry of the pump.

They are calculated experimentally, for a speed from the characteristics of the height, power, and performance as a function of the pump flow rate.

3. Control Laws

3.1. MPPT Control

The optimal power of the PV Generator fluctuates with the climatic conditions, solar flux, temperature and wind speed. The coupling charging with constant power, without using batteries, can not ensure an optimum operation. Therefore, it is essential to provide a power adapter to support the power from the PV generator. This action can be done with a PWM (Pulse Width Modulator) control via a DC/DC converter witch is controlled by MPPT (Maxi Power Point Tracking) through its duty-cycle.

3.2. The Control Law V/f

The relationship of the output voltage-to-frequency (V/f) can be set to constant or variable, depending on the load request, the inverter frequency, the external climatic disturbances and conditions. At the startup, the relationship V/f increases in a short time to enrich the instantaneous starting current of the moto-pump.

4. Simulation Results

The meteorological parameters, especially temperature and solar irradiation, are not constant throughout the day, and they vary considerably. To observe the influence of these factors on the different characteristics of the system given in Figure 1, we performed simulations for several couples of illuminance, solar energy and temperature. The characteristics of the PV plan are as follows:

- Power plant: 3 kW
- PV Solar cell : monocristalline
- Nominal Power of each panel: 250 W
- Short circuit current: 4.75 A
- Open circuit voltage: 63 V
- Efficiency: 18.6%
- Operating Temperature Range: -25 to 75°C
- Number of panels = 12 (6 serial & 2 parallel)
- Three-phase inverter 3 kVA, 12–127 V, 5–60 Hz
- Motor pump group composed of a three-phase asynchronous motor 2 kW, 3 phases of 127 V, 50 Hz and a centrifugal pump submersible ($H_n = 65$ m).

4.1. Optimal Irradiation of 1000 W/m^2 and 25°C

We illustrated in Figures 2–4 some simulation results, including the flow rate of the pump, the motor speed and the maximum power provided by the PV generator for weather data equal to 1000 W/m^2 and 25°C .

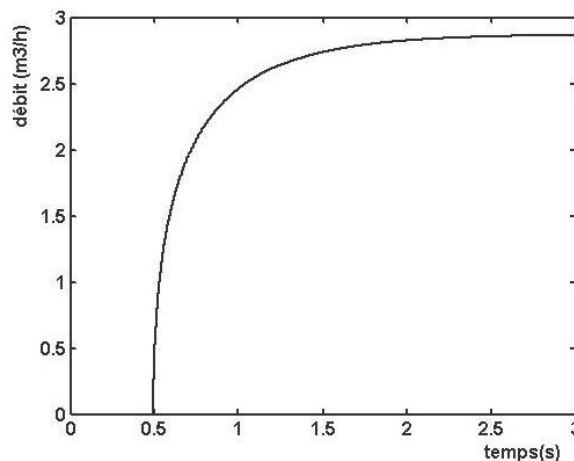


Figure 2. Variation of the flow rate of the pump as a function of temperature ($\varnothing = 1000 \text{ W/m}^2$ and $T_a = 25^{\circ}\text{C}$).

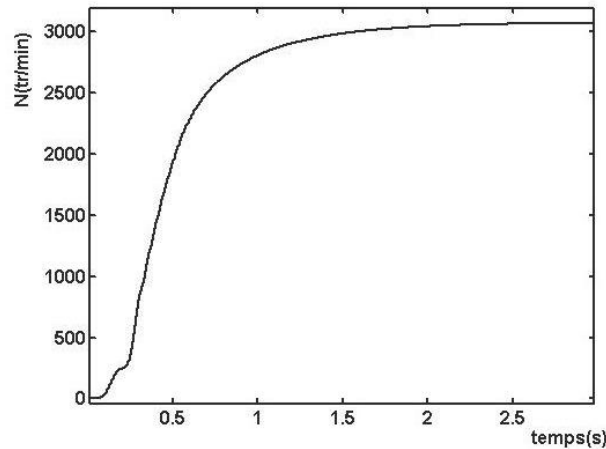


Figure 3. Speed variation of the motor as a function of temperature ($\varnothing = 1000 \text{ W/m}^2$ and $T_a = 25 \text{ }^\circ\text{C}$).

Figure 4 shows that the maximum power provided by the generator is 1800 W. This shows the reliability of the control law in MPPT calculated around the DC/DC. It is also noted that the flow rate of the pump as well as the speed of the machine are optimal. This shows the reliability of the control V/f computed around the DC/AC.

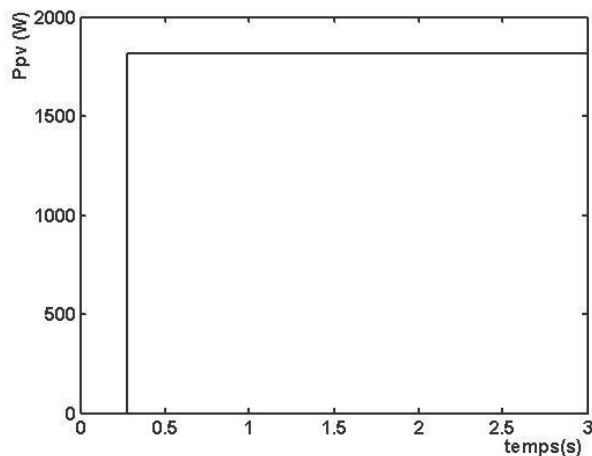


Figure 4. Variation of the maximum power of the PV generator as a function of temperature ($\varnothing = 1000 \text{ W/m}^2$ and $T_a = 25 \text{ }^\circ\text{C}$).

4.2. Disturbed Responses

The results of simulation of the PV pumping system are recorded in Figures 5–8 under the real-time disrupted weather conditions. Especially, the variation of motor speed and the pump flow. The pumping functioning point requires a static value of voltages and currents and a sufficient power which exceeds 1700 W. For example, we can observe in Figure 6, that the pump can only start from the threshold of 1500 W which corresponds to a speed of 2000 tr/mn. This occurs after a delay time of 1 to 3 s.

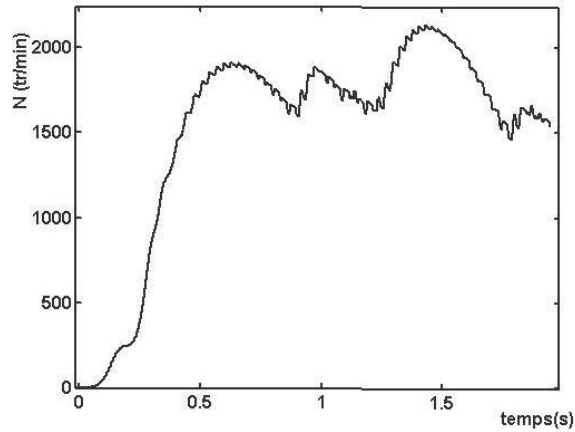


Figure 5. Variation of the speed of the machine for weather interference data.

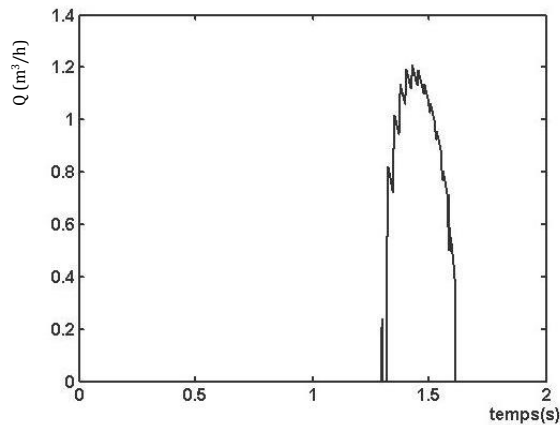


Figure 6. Variation of the pump flow rate for weather interference data.

For the data on weather variables, it is noted that the pump produces a flow of water at speeds above 1800 rpm. The speed of the machine is infected by interference whenever there is a change in temperature and solar radiation.

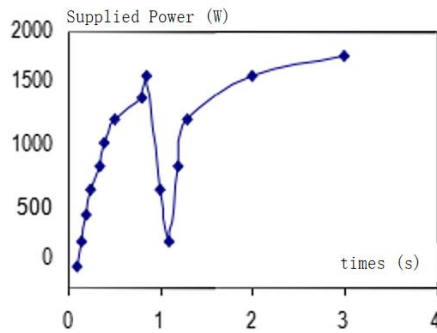


Figure 7. Variation of the supplied power with weather interference data.

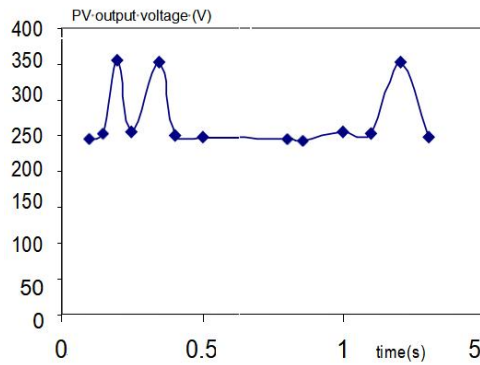


Figure 8. Voltage of the PV generator with weather interference.

4.3. Influence of Temperature

Simulation results are performed in Figures 9–15, including current, frequency, output power, flow rate and global efficiency, for different temperature values from 5 to 75 °C, keeping solar irradiance constant at 1000 W/m².

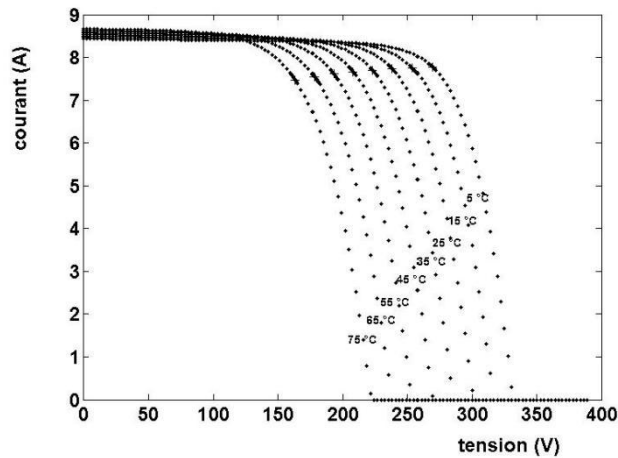


Figure 9. The I-V curve of the PV generator for different Temperatures for $\varnothing = 1000 \text{ W/m}^2$.

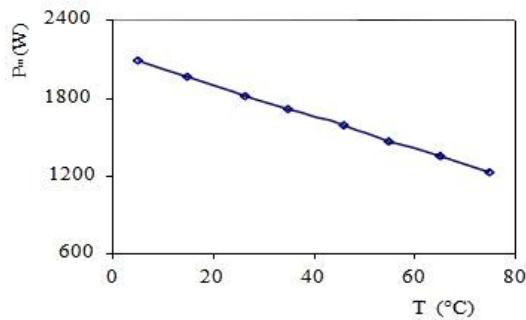


Figure 10. Variation of the power PV with temperature for $\varnothing = 1000 \text{ W/m}^2$.

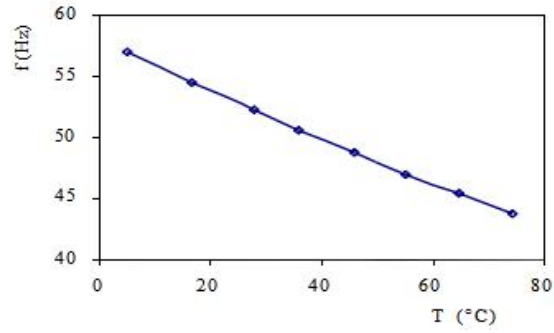


Figure 11. Variation of the frequency with temperature for $\varnothing = 1000 \text{ W/m}^2$.

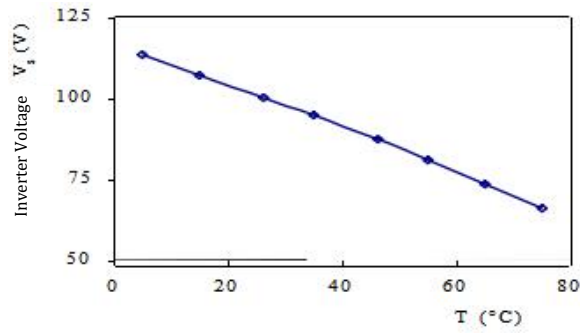


Figure 12. Variation of the voltage of the inverter with temperature for $\varnothing = 1000 \text{ W/m}^2$.

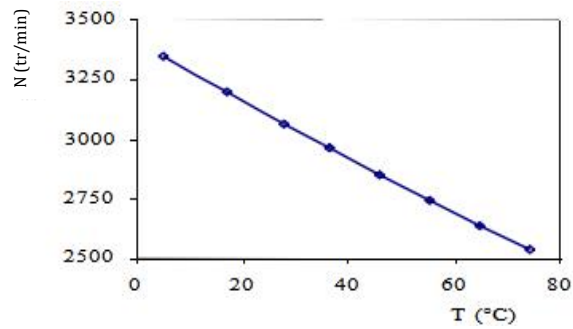


Figure 13. Variation of the speed of the MAS with temperature for $\varnothing = 1000 \text{ W/m}^2$.

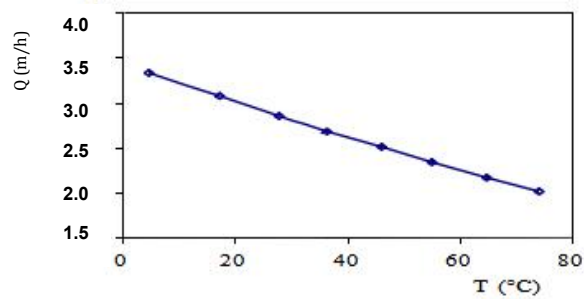


Figure 14. Variation of the pumpflow rate with temperature for $\varnothing = 1000 \text{ W/m}^2$.

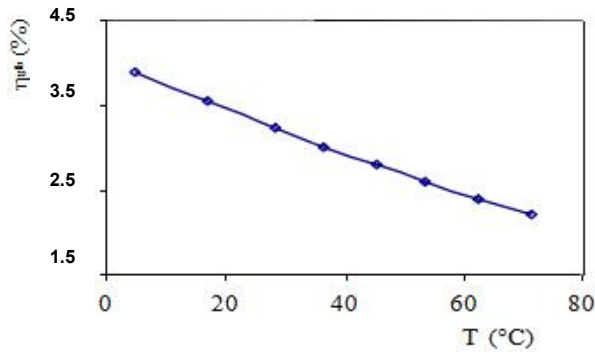


Figure 15. Variation of the overall efficiency of the PV pumping plant with temperature for $\varnothing = 1000 \text{ W/m}^2$.

The changes generated by the latter different curves of the system shown in Figures 9–15 are inversely proportional to the temperature at a specific value of radiation maintained at 1000 W/m^2 . The maximum power provided by the PV generator controlled by MPPT is decreasing at a rate of $12.5 \text{ W/}^\circ\text{C}$, which leads to a reduction of the engine speed and consequently a decrease in pump speed.

The voltage and the output frequency of the inverter also decrease respectively from $0.7 \text{ V/}^\circ\text{C}$ and $0.2 \text{ Hz/}^\circ\text{C}$. As the temperature rises above $25 \text{ }^\circ\text{C}$, this evolution and decrease will result in a $0.03\%/^\circ\text{C}$ decrease in the overall performance of the PV system.

4.4. Influence of Solar Irradiation

In order to show the influence of solar irradiance on the characteristics of the pumping system, we conducted other simulations for different solar irradiance values from 100 to 1000 W/m^2 , keeping the constant temperature at $25 \text{ }^\circ\text{C}$.

The main characteristics of the PV system under several solar irradiance values are illustrated in Figures 16–22.

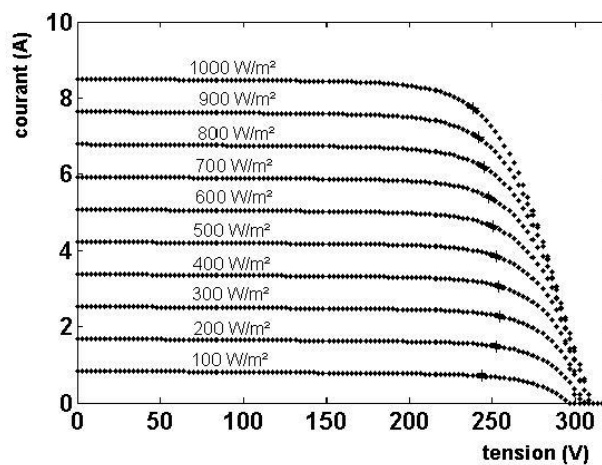


Figure 16. The curve I-V of the PV generator for different solar radiation at $T_a = 25 \text{ }^\circ\text{C}$.

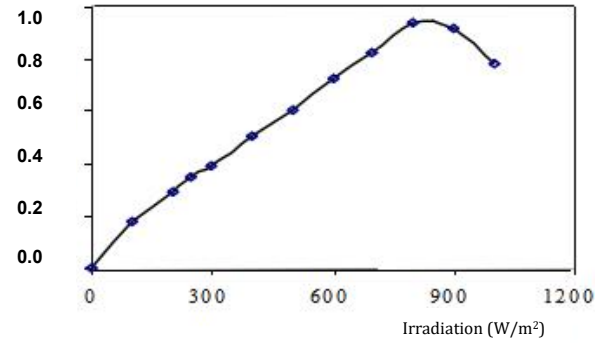


Figure 17. Variation of the factor of adaptation with solar irradiation for $T_a = 25\text{ }^\circ\text{C}$.

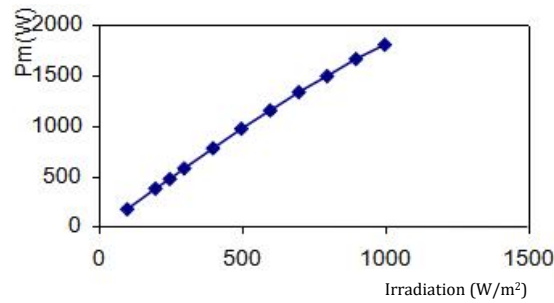


Figure 18. Variation of the power PV with solar irradiation for $T_a = 25\text{ }^\circ\text{C}$.

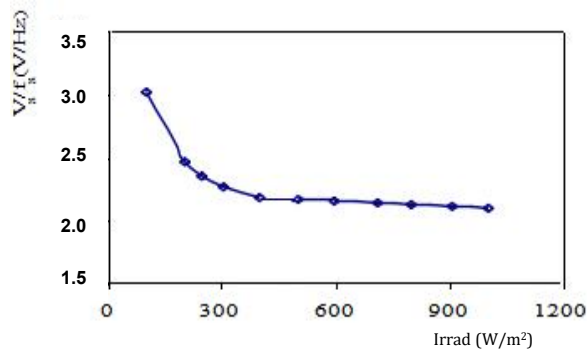


Figure 19. Variation of the control law V/f with solar irradiation.

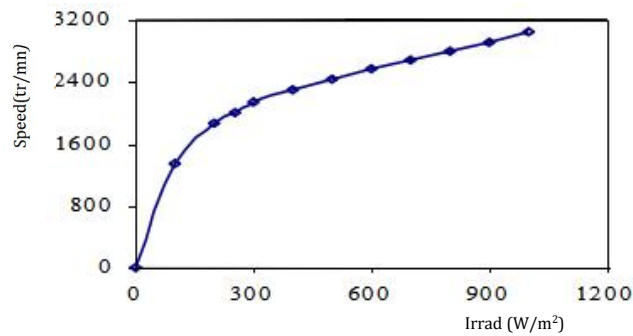


Figure 20. The motor speed variation of the MAS with solar irradiation for $T_a = 25\text{ }^\circ\text{C}$.

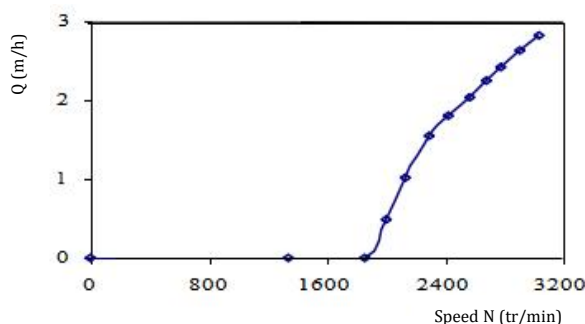


Figure 21. Variation of the pump flow rate with the velocity for $T_a = 25\text{ }^\circ\text{C}$.

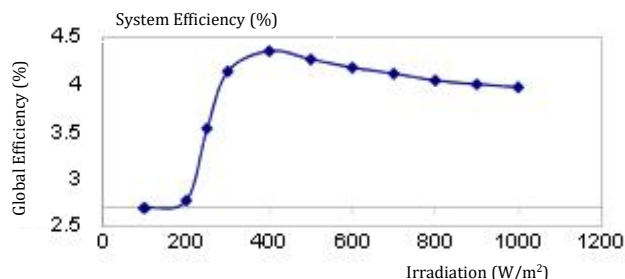


Figure 22. Variation of the overall efficiency with solar irradiation for $T_a = 25\text{ }^\circ\text{C}$.

Different sizes of the pumping system PV, which are illustrated in the last figures, evolve in proportion to solar irradiation and for a constant temperature.

The maximum power provided by the PV generator controlled by MPPT is linear with the light intensity. The power reaches the maximum value for the irradiance of 1000 W/m^2 .

When the solar flux is low and less than 450 W/m^2 , the V/f ratio shows the system can operate in a significant way even during periods of low sunlight. According to Figure 21, the pump starts to generate a flow from a speed motor of 1900 tr/min. This speed is obtained for a minimum illuminance of 250 W/m^2 . The maximum flow rate is $2.8\text{ m}^3/\text{h}$ at an irradiance of 1000 W/m^2 and a constant temperature of $25\text{ }^\circ\text{C}$. The overall yield increases with the illumination from 3% to 4.5%.

These results are compared with other published works [15] and demonstrated their reliable behavior.

5. Discussion

In previous articles, the theoretical and fundamental aspects, such as the choice of the plant structure, the equation of each part and the simulation, were introduced [16]. Not focusing on the modeling details, this paper makes a summary of parametric analysis of previous studies. In this paper, we have presented the system's dynamic behavior and its variation in energy and electrical variables (temperature, solar irradiation, current, voltage, frequency, power, energy consumption, pump flow, global energy efficiency, etc.) of the PV pumping system under different climate conditions and loads.

Also, there are two problems of photovoltaic systems: the intermittency of the source and its random behavior, and the unpredictable variation of the user load and consumption that depend on user behavior. The two factors greatly influence the efficiency of the overall PV system and its stability. It is the problem that is addressed in this study by examining the impacts of these two factors on the PV system behavior and the variations of current, voltage, power and consumption.

The contribution of this paper is as follows:

- Evaluation of the disturbance effects on all parameters and quantities, whether electrical or energetic, and identification of pumping operating thresholds.
- Quantification of the effects of control laws: PWM, VF (Voltage under Frequency) and MPPT.

An example we found in the figures is that the pumping system starts to operate for a solar irradiation of 250 W/m^2 at a reduced speed of 1600 rpm (trs/min) and an overall efficiency of 50%. For 450 W/m^2 , it reaches

its permanent state at a flow rate of 2 m³/h and a motor speed of 2000 rpm. Full speed is reached for 1000 W/m² at a flow rate of 3 m³/hour and a motor speed of 2800 rpm.

This result is important because it can predict the optimal operation period of the pumping system for future control through IoT and AI in the case of intelligent climate agriculture, which will be the subject of our next study.

The limitations of this study are:

- The problem of electric storage, especially during rainy and cloudy critical conditions, for rural plants which are far from the grid, and follow standalone structures.
- The non-linearity of the system which imposes specific controls.
- Absence of a precise mathematical model for estimating the load based on the application.
- Variation in frequency in the event of an imbalance between the supplied power and the required power provided by the load, which affects all electrical quantities and can lead to a shutdown of the installation to protect the converters and components of the PV system.

Furthermore, this study is one of the rare studies that visualize the effects on all the electrical and energy parameters of the entire system, which allows for the deduction of the daily operating thresholds and margins of the pump to better, manage and predict the system.

6. Conclusions

This study demonstrates the importance of considering the temperature and solar irradiation effects in the design and operation of photovoltaic pumping systems, and provides valuable tools and information for improving their performance and reliability in real scenarios.

Through the development of accurate mathematical models, including electrical models of photovoltaic modules, hydraulic models of pumps, and models of integrated systems, it is possible to quantify and predict the effects of these environmental factors on system performance.

Recent progress in the field of advanced control and supervision has made it possible to implement reliable and robust control laws, capable of adapting to changes in temperature and irradiation levels. However, there is still room for improvement in model refinement, experimental verification and development.

The combined effects of temperature and solar irradiation variations on the performance of photovoltaic pumping systems can be summarized as follows:

- **Decreased Efficiency:** High temperatures reduce the overall efficiency of PV modules, leading to lower power output and reducing pump functioning periods. This can impact the pumping system's ability to meet the requirements of flow rates and water delivery.
- **Output Fluctuations:** Variations in solar irradiation levels can result in fluctuations in the output power of the PV system. This will affect the stability and reliability of the pumping system, especially when solar irradiation levels are low.
- **System Sizing and Design:** Accurate estimation of the available solar resources and consideration of temperature effects are crucial to ensure optimal system performance and reliability.
- **Energy Storage and Backup:** Batteries, backup power sources or hydraulic storage can be integrated into the system. Energy storage allows for the utilization of excess power under optimal conditions and provides backup power during periods of low solar irradiation or high energy demand.

Author Contributions

M.J: Conceptualization, methodology, simulation and writing; A.C: Supervision, validation and correction. All authors have read and agreed to the published version of the manuscript.

Funding

This work received no external funding.

Institutional Review Board Statement

Not applicable.

Informed Consent Statement

Not applicable.

Conflicts of Interest

The authors declare no conflict of interest.

References

1. Cherif, A. Modelling and Simulation of Photovoltaic Refrigeration System with Latent Storage. PhD thesis, University of Tunis Manar, Tunisia, 1997.
2. Sontake, V.C.; Kalamkar, V.R. Solar photovoltaic water pumping system - A comprehensive review. *Renewable Sustainable Energy Rev.* **2016**, *59*, 1038–1067. [[CrossRef](#)]
3. Soon, J.J.; Low, K.-S. Optimizing Photovoltaic Model for Different Cell Technologies Using a Generalized Multidimension Diode Model. *IEEE Trans. Ind. Electron.* **2015**, *62*, 6371–6380. [[CrossRef](#)]
4. Hysa, A. Modeling and Simulation of the Photovoltaic Cells for Different Values of Physical and Environmental Parameters. *Emerging Sci. J.* **2019**, *3*, 395–406. [[CrossRef](#)]
5. Metwally, H.M.B.; Anis, W.R. Performance analysis of PV pumping systems using switched reluctance motor drives. *Sol. Energy* **1996**, *56*, 161–168. [[CrossRef](#)]
6. Duffie, J.A.; Beckman, W.A. *Solar Engineering of Thermal Processes*, 4th ed.; John Wiley & Sons, Inc.: Hoboken, New Jersey, USA, 2013; 928p. [[CrossRef](#)]
7. Hossain, M.S.; Pandey, A.K.; Rahim, N.A.; Selvaraj, J.; Tyagi, V.V.; Islam, M.M. Self-cleaning Assisted Photovoltaic System with Thermal Energy Storage: Design and Performance Evaluation. *Sol. Energy* **2020**, *206*, 487–498. [[CrossRef](#)]
8. Makenzi, M., Muguthu, J.; Murimi, E. Novel Design and Sizing Approach for Optimal Installation of Solar Water Pumping Setups. *Appl. Sol. Energy* **2022**, *57*, 391–402. [[CrossRef](#)]
9. Chandel, S.S.; Naik, M.N.; Chandel, R. Review of Performance Studies of Direct Coupled Photovoltaic Water Pumping Systems and Case Study. *Renewable Sustainable Energy Rev.* **2017**, *76*, 163–175. [[CrossRef](#)]
10. Mellit, A.; Kalogirou, S.A.; Hontoria, L.; Shaari, S. Artificial Intelligence Techniques for Sizing Photovoltaic Systems: A Review. *Renewable Sustainable Energy Rev.* **2009**, *13*, 406–419. [[CrossRef](#)]
11. Jraidi, M. Modeling and Control of a Pumping System. PhD Thesis, University of Tunis Manar, Tunisia, 2005.
12. Hamrouni, N. Modelling, Simulation and Control of a PV Pumping System. In Proceedings of 8th International Conference on Modeling and Simulation of Electric Machines, Converters and Systems, Hammamet, Tunisia, 17–20 April 2005.
13. Labrique, F.; Segulier, G.; Bausière, R. *Les Convertisseurs de l'électronique de puissance. Tome 4, La conversion continu - alternatif*; ISBN 978-2-7430-0035-6.
14. Hamrouni, N.; Jraidi, M.; Cherif, A.; Dhoub, A. Measurements and Simulation of a PV Pumping Systems Parameters Using MPPT and PWM Control Strategies. In Proceedings of the 2006 IEEE Mediterranean Electrotechnical Conference, Malaga, Spain, 16–19 May 2006. [[CrossRef](#)]
15. Habib, S.; Liu, H.; Tamoor, M.; Zaka, M.A.; Jia, Y.; Hussien, A.G.; Zawbaa, H.M.; Kamel, S. Technical modelling of solar photovoltaic water pumping system and evaluation of system performance and their socio-economic impact. *Heliyon* **2023**, *9*, 1–24. [[CrossRef](#)]
16. Hamrouni, N.; Younsi, S.; Jraidi, M. Modelling, Command and Treatment of a PV Pumping System Installed in Tunisia. *Int. J. Adv. Comput. Sci. Appl.* **2019**, *10*, 414–420. [[CrossRef](#)]



Copyright © 2024 by the author(s). Published by UK Scientific Publishing Limited. This is an open access article under the Creative Commons Attribution (CC BY) license (<https://creativecommons.org/licenses/by/4.0/>).

Publisher's Note: The views, opinions, and information presented in all publications are the sole responsibility of the respective authors and contributors, and do not necessarily reflect the views of UK Scientific Publishing Limited and/or its editors. UK Scientific Publishing Limited and/or its editors hereby disclaim any liability for any harm or damage to individuals or property arising from the implementation of ideas, methods, instructions, or products mentioned in the content.